Effect of the Flow Rates in Linear, Ideal, Simulated Moving-Bed Chromatography

Guoming Zhong, Maureen S. Smith, and Georges Guiochon
Dept. of Chemistry, University of Tennessee, Knoxville, TN 37996
Div. of Chemical and Analytical Sciences, Oak Ridge National Laboratory, Oak Ridge, TN 37831

The algebraic solution for linear, ideal simulated moving-bed (SMB) chromatography derived previously revealed important new properties of the SMB process. This solution was validated by comparing with experimental data and with the results of numerical solutions of the equilibrium–dispersive and the lumped kinetic model. This earlier solution, however, was limited to the simple case in which the safety factor was assumed to be the same for the flow rates in all four sections. An extension of this solution to the case in which the safety factors differ and allow an independent selection of the four different flow rates (within limits) is derived. This solution accounts well for most practical situations. It permits the discussion of the influence of different flow rates on the performance of an SMB unit, an issue of critical importance for the optimization of the design and operation of these separators.

Introduction

Simulated moving-bed chromatography (SMB) is an important separation process that implements countercurrent chromatography. It has long been recognized that the latter process is impractical because the backward migration of the solid phase would cause its rapid degradation by erosion as well as considerable remixing, hence poor separation efficiency. In SMB, the backward migration of the solid phase is simulated by periodic switching of the inlets of the feed and solvent and of the outlets of the raffinate and extract. Figure 1 illustrates the principle of the Sorbex process (Broughton, 1985). A set of identical columns is used. The periodic switching of the four ports in the direction of the liquid stream simulates the backward migration of the solid phase by periodic backward leaps equal to one column length. The choice of an appropriate period provides the required solid-phase velocity. Thus, a simulated countercurrent is achieved and the drawbacks associated with the physical movement of the solid phase are avoided. The process is continuous, can separate a binary feed into two highly purified fractions with complete recovery, may separate effectively compounds having a relatively small separation factor, and has been used for a variety of industrial applications (Broughton, 1985).

However, SMB has remained long shrouded in secrecy because of its proprietary nature (Broughton and Gerhold, 1961), because of the complexity of the implementation that makes it difficult to build at the laboratory scale for academic investigations (Broughton et al., 1970), and because of the limited number of its applications (Broughton, 1985). However, it has been realized recently that this process is uniquely suited to the production of pure enantiomers (Stinson, 1995). In the last ten years, we have come to realize that the metabolism of the two enantiomers of a compound in living cells is often profoundly different. The FDA has decided to consider the two enantiomers as two different chemicals for the purpose of their approval as drugs (Anon., 1992). The pharmaceutical industry needs a general process for the separation of enantiomers at the pilot level (to produce pure enantiomers for validation-related work and for animal and clinical tests) as well as at the production level (Stinson, 1995). The pesticide industry is now realizing that the two enantiomers of a conventional insecticide may have quite different toxicity and that their toxicity ratios for pests and for mammals, including humans, are often quite different. In the best cases, we can achieve the same degree of plant protection for half the environmental load.

Accordingly, considerable attention is devoted to the SMB process, and attempts are made at operating and optimizing small units for a variety of batch productions. Production runs being short, optimization procedures are searched that require fewer successive trials and incorporate more theoretical

Correspondence concerning this article should be addressed to G. Guiochon.

knowledge and less empiricism. Recently, we have derived an algebraic solution of the general model of the conventional Sorbex SMB under a set of restrictive conditions: (1) for the ideal, linear model; (2) for a four-column (i.e., one column per section) unit; and (3) with the same safety factor for the liquid flow rates in all four sections (Zhong and Guiochon, 1996). The study of this solution has shown some properties ignored so far, such as the existence of oscillations on the plateaus of the raffinate and extract concentration profiles in their corresponding sections. It has allowed the direct calculation of the properties of the asymptotic steady state as the limits of infinite series or products. This simple solution is easy to use since its implementation requires only a pocket calculator or a spreadsheet.

The use of the ideal, linear model to investigate, let alone optimize, the performance of an SMB separator requires some justification. The use of linear, noncompetitive isotherms for the two feed components is justified by the fact that this simple isotherm applies to at least two important industrial applications of SMB, the separation of glucose and fructose [Sarex process (Broughton, 1985)] and that of light olefins and paraffins [C4 fraction, Olex process (Broughton, 1985)]. In the former case, several groups have reported that the equilibrium isotherms of these sugars on ion-exchange resins were linear (Ching and Ruthven, 1985; Balannec and Hotier, 1994). Howard et al. (1988) reported it to be linear up to at least 200 g/L. Similarly, Barker et al. (1983) found linear isotherms in the study of the separation of high molecular-weight dextranes on silicagel, using size exclusion chromatography. In the second case, Johnson and Kabza (1994) suggested linear isotherms in a wide range of concentrations. Certainly, the applications of SMB currently being developed in the pharmaceutical industry, for example, the separation of enantiomers, will often require that operations be carried out under nonlinear conditions. However, Maki (1994) reported the separation of glutathione and glutamic acid on a cation exchange resin under linear conditions, and Küsters et al. (1995) separated two enantiomers under near linear conditions (in this last case, the maximum concentration used is set by the low solubility of the feed). Even under nonlinear conditions, a number of properties of the solution obtained under linear conditions can be extended, for example, the existence of oscillations on the concentration plateaus obtained with efficient columns, which are required for these difficult separations (the separation factor of enantiomers rarely exceeds 1.4 and is often around 1.2).

The use of the ideal model allows the separation of the influence of the fundamental flow and thermodynamic phenomena from that of axial apparent dispersion. It is considered as the first approximation for the calculation of the behavior of chromatographic systems (Helfferich and Klein, 1970). The ideal model gives the position of concentration profiles or the time of the concentration histories. Actual band profiles differ from these derived from the ideal model only by an amount of dispersion depending on the efficiency of the columns used. Because, under linear conditions, this dispersion amounts to a convolution with a Gaussian function, the difference between actual band profiles and ideal ones is predictable. As a matter of fact, the algebraic solution of the ideal, linear model of SMB has been validated by comparison of its results with experimental data (Yun et al., 1997a). Concentration profiles acquired with an SMB unit having columns of moderate efficiency ($N \simeq 800$ theoretical plates) agree well with the predictions of the algebraic solution, except for the expected amount of axial dispersion taking place with columns of finite efficiency. Excellent agreement was also reported with the results of numerical solutions performed under various sets of experimental conditions (Zhong and Guiochon, 1996).

The main purpose of this work is a discussion of the influence of separate changes of the four flow rates in an SMB unit on its performance. This requires the derivation of an extension of the algebraic solution to the case in which the liquid flow rates in the four different sections have different safety factors, hence can be adjusted separately within some limits to be discussed. The proper adjustment of these four flow rates is an important practical aspect of the optimization of the operation of an SMB separation that has to be carried out by trials and errors. The validation of the present work is presented in a separate paper (Yun et al., 1997b).

Model of Simulated Moving Bed

We consider a basic Sorbex system of SMB, shown in Figure 1. It consists of four identical columns. The countercurrent migration of the solid phase, which is maintained stationary inside fixed columns, is simulated by switching periodically the solvent, feed, and drawoff ports in the direction of the liquid-phase flow. The apparent velocity of the solid phase is the same in each column because it depends only on the volume of solid phase in the column and on the switching time (as will be discussed later).

Column model

The differential mass balance in column j, for component i in an ideal (i.e., equilibrium) model is written:

$$\frac{\partial C_{i,j}}{\partial t} + u_j \frac{\partial C_{i,j}}{\partial z} + F \frac{\partial q_{i,j}}{\partial t} = 0, \tag{1}$$

where $C_{i,j}$ and $q_{i,j}$ are the liquid- and solid-phase concentrations of component i in column j; u_j is the liquid phase velocity; $F = (1 - \epsilon)/\epsilon$ is the phase ratio; and ϵ is the column total porosity. Since we consider the separation of a binary mixture and a four column SMB system, $i = 1, 2$ and $j =$ I, II, III, IV.

A linear adsorption equilibrium is considered, with

$$q_{i,j} = K_i C_{i,j}. \tag{2}$$

Component 1 is assumed to be less retained than component 2 in the column, that is, $K_1 < K_2$. The separation factor is $\alpha = K_2/K_1 > 1$.

The initial and boundary conditions of the problem are:

$$C_{i,j}(x,0) = 0, \qquad q_{i,j}(x,0) = 0 \tag{3a}$$

$$C_{i,j}(0,t) = C_{i,j}^{\text{in}}, \quad q_{i,j}(0,t) = f_i\left(C_{1,j}^{\text{in}}, C_{2,j}^{\text{in}}\right) \tag{3b}$$

where $C_{i,j}^{\text{in}}$ is the concentration of component i at the inlet of

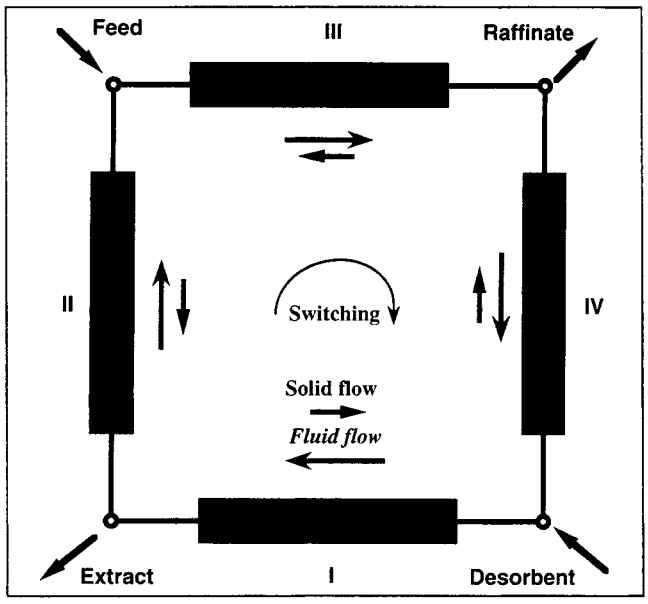

Figure 1. Sorbex SMB.

column j, concentration that is related to the node flow and to the mass-balance equations. These conditions are updated at the beginning of each new cycle.

Node model

The flow and integral mass-balance equations at each node are given by the following equations (Ruthven and Ching, 1989) in which Q_{I}, Q_{II}, Q_{III}, Q_{IV} are the flow rates through the corresponding columns; Q_D is the desorbent flow rate; Q_E, the extract flow rate; Q_F, the feed flow rate; and Q_R, the raffinate flow rate:

Desorbent node (eluent):

$$Q_{\mathrm{IV}} + Q_D = Q_{\mathrm{I}}$$
$$C^{\mathrm{out}}_{i,\mathrm{IV}} Q_{\mathrm{IV}} + C_{i,D} Q_D = C^{\mathrm{in}}_{i,\mathrm{I}} Q_{\mathrm{I}}. \tag{4a}$$

Extract drawoff node:

$$Q_{\mathrm{I}} - Q_E = Q_{\mathrm{II}}$$
$$C^{\mathrm{out}}_{i,\mathrm{I}} = C^{\mathrm{in}}_{i,\mathrm{II}} = C_{i,E}. \tag{4b}$$

Feed node:

$$Q_{\mathrm{II}} + Q_F = Q_{\mathrm{III}}$$
$$C^{\mathrm{out}}_{i,\mathrm{II}} Q_{\mathrm{II}} + C_{i,F} Q_F = C^{\mathrm{in}}_{i,\mathrm{III}} Q_{\mathrm{III}}. \tag{4c}$$

Raffinate drawoff node:

$$Q_{\mathrm{III}} - Q_R = Q_{\mathrm{IV}}$$
$$C^{\mathrm{out}}_{i,\mathrm{III}} = C^{\mathrm{in}}_{i,\mathrm{IV}} = C_{i,R}. \tag{4d}$$

In these equations, $C^{\mathrm{out}}_{i,j}$ and $C^{\mathrm{in}}_{i,j}$ are the concentrations of component i at the outlet and inlet of column j, respectively. Q_j is the flow rate through column j. It is related to the liquid-phase velocity, u_j, by $Q_j = \epsilon A u_j$, where A is the column cross-section area, which is assumed, without loss of generality, to be the same for all the columns, including the feed and drawoff columns.

Separation condition

Following the studies by Ruthven and Ching (1989) and Zhong and Guiochon (1996), complete separation of a binary mixture and stable operation of the SMB unit are achieved if eight inequalities are satisfied. These inequalities are relative to the values of the ratio between the mass flow rates of components 1 and 2 in the solid and the fluid phases in each of the four-column sections. The solid-phase flow rate (Q_S) is created by the relative apparent movement of this phase caused by column switching. It is derived from the fraction of the column volume in one column occupied by the solid and from the switching time:

$$Q_S = (1-\epsilon) A u_s = \frac{(1-\epsilon) AL}{t^*}, \tag{5}$$

where A is the geometrical area of the column cross-section, L its length, and t^* is the switching time. These inequalities can be reduced to only four because $\alpha > 1$, so in columns I and III the more strongly adsorbed component is the critical component, while in columns II and IV it is the less adsorbed component that is the critical one.

Following Ruthven and Ching (1989), we define four critical net mass flow rate ratios, β_j ($\beta_j > 1$, $j = 1, \ldots, 4$), all defined to be larger than unity. In sections III and IV, β_j is the ratio of the solid to the net liquid phase flow rates, for components 2 and 1, respectively. In sections I and II, β_j is the reverse, or ratio of the net liquid- to the solid-phase flow rates, for components 2 and 1, respectively. These definitions arise from the basic condition of stability of the SMB, that the two feed components move in opposite directions in each section, and from the fact that, if the critical condition in each section is met, the other condition is also met (Ruthven and Ching, 1989; Zhong and Guiochon, 1996). Since the solid-phase flow rate is based on the column length and switching time (see Eq. 5), it is constant in all four sections, since four identical columns must be used. Thus, increasing the value of β requires an increase of the liquid phase flow rate in sections I and II and a decrease of the liquid phase flow rate in sections III and IV. This observation will be useful for the later discussion of the influence of the flow rate on the SMB performance.

From these definitions and Eqs. 4a–4d, we derive the following relationships:

$$Q_{\mathrm{I}}/Q_S = K_2 \beta_1 + 1/F \tag{6a}$$
$$(Q_{\mathrm{I}} - Q_E)/Q_S = K_1 \beta_2 + 1/F \tag{6b}$$
$$(Q_{\mathrm{I}} - Q_E + Q_F)/Q_S = K_2/\beta_3 + 1/F \tag{6c}$$
$$(Q_{\mathrm{I}} - Q_E + Q_F - Q_R)/Q_S = K_1/\beta_4 + 1/F. \tag{6d}$$

In our previous publication, the same factor β was used for all four sections. This restricts the generality of the conclusions derived because, once β is chosen, all the flow rates

(raffinate, extract, desorbent, flow rates in each section) are fixed with respect to the feed flow rate. A relaxation of this condition is necessary, because, in practice, it is necessary to change these flow rates to make any SMB system work and to optimize it. The influence of the different flow rates on the performance is a most important issue of SMB research.

The system of algebraic linear equations written earlier (Eqs. 6a–6d) can easily be rearranged as follows

$$Q_F = \left(\frac{K_2}{\beta_3} - K_1\beta_2\right)Q_S \tag{7a}$$

$$Q_E = (K_2\beta_1 - K_1\beta_2)Q_S \tag{7b}$$

$$Q_R = \left(\frac{K_2}{\beta_3} - \frac{K_1}{\beta_4}\right)Q_S \tag{7c}$$

$$Q_D = \left(K_2\beta_1 - \frac{K_1}{\beta_4}\right)Q_S. \tag{7d}$$

To operate an SMB system, we need all the flow rates to be positive. This can be translated into the following conditions

$$\beta_2\beta_3 < \alpha \tag{8a}$$

$$\beta_2/\beta_1 < \alpha \tag{8b}$$

$$\beta_3/\beta_4 < \alpha \tag{8c}$$

$$\beta_1/\beta_4 < \alpha. \tag{8d}$$

However, a close examination of this set of equations, explicating all the $\beta_j > 1$, results in the conclusion that only Eq. 7a is necessary (Yun et al., 1997b).

Analytical Solution

Axial band profiles

In a previous study (Zhong and Guiochon, 1996), we showed that the system of equations presented in the previous section has an algebraic solution. Because the model is ideal, there is no axial dispersion, and the front and rear of each component profile is staircase. The solution gives algebraic equations to calculate the height and location of each step of these staircases. The following three ratios between the flow rate in the four sections of an SMB with the same β value are important parameters of this algebraic solution. These ratios, which characterize completely the linear, ideal SMB system, will also be most useful in writing the algebraic solution of an SMB with different values of β_j in each section. In this case, they become

$$K_A = \frac{Q_{II}}{Q_{III}} = \frac{1+FK_1\beta_2}{1+FK_2/\beta_3} < 1 \tag{9a}$$

$$K_B = \frac{Q_{IV}}{Q_{III}} = \frac{1+FK_1/\beta_4}{1+FK_2/\beta_3} < 1 \tag{9b}$$

$$K_C = \frac{Q_{II}}{Q_I} = \frac{1+FK_1\beta_2}{1+FK_2\beta_1} < 1. \tag{9c}$$

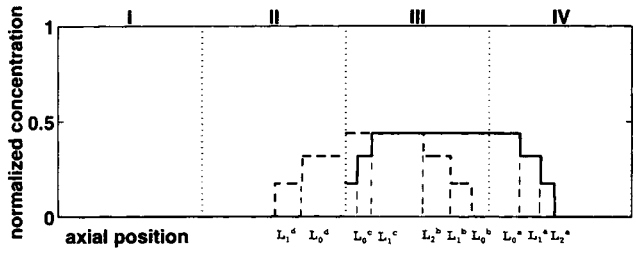

Figure 2. Definitions of the step positions.

Concentration profiles at the end of the third cycle.
Numerical values of the parameters: $K_1 = 2$, $K_2 = 4$, $F = 0.5$, $Q_F = 1.0$ mL/min, $C_{1,F} = C_{2,F} = 1$ mg/mL.
Solid line: raffinate (component 1); dotted line: extract (component 2). $\beta_1 = \beta_2 = \beta_3 = \beta_4 = 1.2$. Ordinate: concentrations normalized to the corresponding feed concentration; abscissa: axial position normalized to the column length.

Following the approach used in our previous work (Zhong and Guiochon, 1996), we calculate the concentration profiles of the two components along the four sections of the SMB and their concentration histories at the raffinate and extract drawoff ports. The concentration histories at the drawoff ports are mere transformations of the concentration profiles along the columns, from the space domain into the time one. Thus, they are only briefly discussed in this study. Note that the axial concentration profiles along the columns are all represented at the end of a cycle, which explains why the raffinate is in sections III and IV, the extract in sections II and III, while there is no feed component in section I, at least when the SMB operates properly.

First, the concentration of the step generated during the nth cycle is

$$C_i^{nt^*} = (1 - K_A^n)C_{i,F}. \tag{10}$$

For reasons explained later, there is only a finite number of vertical steps in each concentration profile.

When a new concentration step appears for the first time in a section (see Figure 2), its position is denoted L_0, with a subscript that denotes the corresponding section. Superscripts a for section IV and c for section III characterize the raffinate profile. Superscripts b for section III and d for section II characterize the extract profile. The respective values of these initial positions are

$$L_0^a = \frac{F(K_2/\beta_3 - K_1)(1+FK_1/\beta_4)}{(1+FK_1)(1+FK_2/\beta_3)}L \tag{11a}$$

$$L_0^b = \frac{FK_2(1-1/\beta_3)}{(1+FK_2)}L \tag{11b}$$

$$L_0^c = \frac{FK_1(\beta_2-1)(1+FK_2/\beta_3)}{(1+FK_1)(1+FK_1\beta_2)}L \tag{11c}$$

$$L_0^d = \frac{F(K_2 - K_1\beta_2)}{(1+FK_2)}L. \tag{11d}$$

These lengths are measured from the inlet of a column, in the direction of migration of the corresponding component. So, if we take the more conventional definition of the inlet of a column as the end through which the solvent enters, L_0^a is measured from the inlet of column (or section) IV, L_0^b is measured from the outlet of column III, L_0^c is measured from the inlet of column III, and L_0^d is measured from the outlet of column II. These definitions are illustrated in Figure 2 for $\beta_j = 1.2$, at the end of the third cycle, just before column switching takes place.

The migration distance of the lowest concentration step ($C_i = 0$ to $C_i = C_i^*$, Eq. 10) during the nth cycle is given by

$$L_{n-1}^a = K_B^{n-1} L_0^a \tag{12a}$$

$$L_{n-1}^b = K_A^{-n+1} L_0^b \tag{12b}$$

$$L_{n-1}^c = K_A^{-n+2} L_0^c \tag{12c}$$

$$L_{n-1}^d = K_C^{n-2} L_0^d. \tag{12d}$$

Figure 2 illustrates this migration for $n = 3$. The abscissa axis gives the axial position along the columns; the ordinate axis gives the ratio of the local concentrations to the feed concentrations.

A step that has been in a section for several cycles, such as m, will have migrated a total distance $\Lambda_m^k = L_0^k + L_1^k + \cdots + L_{m-1}^k$ (k being a, b, c, or d). Because K_A, K_B, and K_C are smaller than 1, both Λ_n^a and Λ_n^d tend toward a finite limit when n increases indefinitely, while neither Λ_n^b nor Λ_n^c does. The asymptotic positions of the front of the raffinate concentration profile in section IV and of the rear of the extract concentration profile in section II are

$$\Lambda_\infty^a = \frac{L_0^a}{1 - K_B} < L \tag{13a}$$

$$\Lambda_\infty^d = \frac{L_0^d}{1 - K_C} < L. \tag{13b}$$

An illustration of the asymptotic concentration profiles is given in Figure 3. Other illustrations of the algebraic solution are also found in the figures shown later. An interesting feature of these solutions is the square oscillation on the concentration plateaus in sections II and IV. The origin of these oscillations has been discussed previously (Zhong and Guiochon, 1996). Because neither Λ_n^b nor Λ_n^c tends toward a finite limit, there are only a limited number of steps in the concentration profiles of both components in section III. A higher step is alternately formed and destroyed during successive cycles. This is the origin of these oscillations. The physical validity of this result has been demonstrated (Yun et al., 1997a).

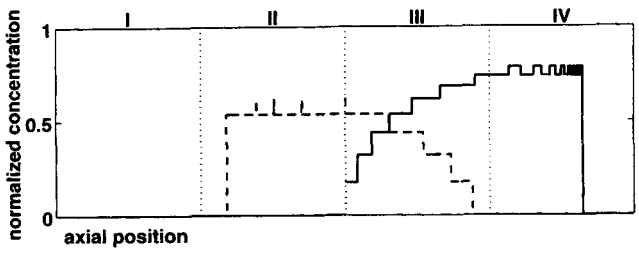

Figure 3. Asymptotic concentration profiles.

Concentration profiles under steady-state conditions. Same flow-rate ratio β in all four sections. Same values of the parameters as in Figure 2. The production rates of the raffinate and extract are shown by the dotted-lines in Figures 5c and 4d, respectively.

Production rates

Following our previous study (Zhong and Guiochon, 1996), the production rates of the raffinate and extract at their corresponding withdrawal ports can be straightforwardly calculated for different values of the flow rates. In fact, they are, respectively, the breakthrough curves of axial profiles along columns IV and II.

Let's define two cycle numbers n_r and n_e when the raffinate and extract reach their maximum concentrations, i.e., they satisfy

$$\Lambda_{n_r}^c \le L < \Lambda_{n_r+1}^c \tag{14a}$$

$$\Lambda_{n_e}^b \le L < \Lambda_{n_e+1}^b. \tag{14b}$$

The average production rate during any cycle n, $n \le n_r$ and n_e, can be written in the following general forms

$$PR(n) = \left(\frac{1 - K_B^n}{1 - K_B} - \frac{K_A^n - K_B^n}{K_A - K_B} K_A \right) \frac{PR(1)}{1 - K_A} \tag{15a}$$

$$PE(n) = \left(\frac{1 - K_C^{n-2}}{1 - K_C} - \frac{K_A^{n-2} - K_C^{n-2}}{K_A - K_C} K_A \right) \frac{PE(3)}{1 - K_A}, \tag{15b}$$

where $PR(1)$ and $PE(3)$ are the first production rates of the raffinate and extract during the first and third cycles, respectively. The first two cycles do not produce any extract:

$$PR(1) = \frac{C_1^* t_0^a Q_R}{t^*} = \frac{F^2 (K_2/\beta_3 - K_1/\beta_4)(K_2/\beta_3 - K_1)}{(1 + FK_2/\beta_3)^2} C_{1,F} Q_F \tag{16a}$$

$$PE(3) = C_2^* t_0^d Q_E / t^* = \frac{F^2 (K_2/\beta_1 - K_1 \beta_2)(K_2 - K_1 \beta_2)}{(1 + FK_2/\beta_3)(1 + FK_2 \beta_1)} C_{2,F} Q_F, \tag{16b}$$

where $C_{1,F}$ is the feed concentration of the raffinate component; $t_0^a = L_0^a / V_{1,\mathrm{IV}}$ is the duration of production; L_0^a is the length of the raffinate concentration plateau inside column IV (see Figure 2); $V_{1,\mathrm{IV}} = u_{\mathrm{IV}}/(1 + FK_1)$ is the propagation velocity of component 1 along column IV; $t_0^d = L_0^d / V_{2,\mathrm{I}}$ is the duration of production; L_0^d is the length of the extract concentration plateau inside column II (see Figure 2); and $V_{2,\mathrm{I}} = u_{\mathrm{I}}/(1 + FK_2)$ is the propagation velocity of component 2 along column I.

After the maximum concentration is reached, the production rates can be expressed as

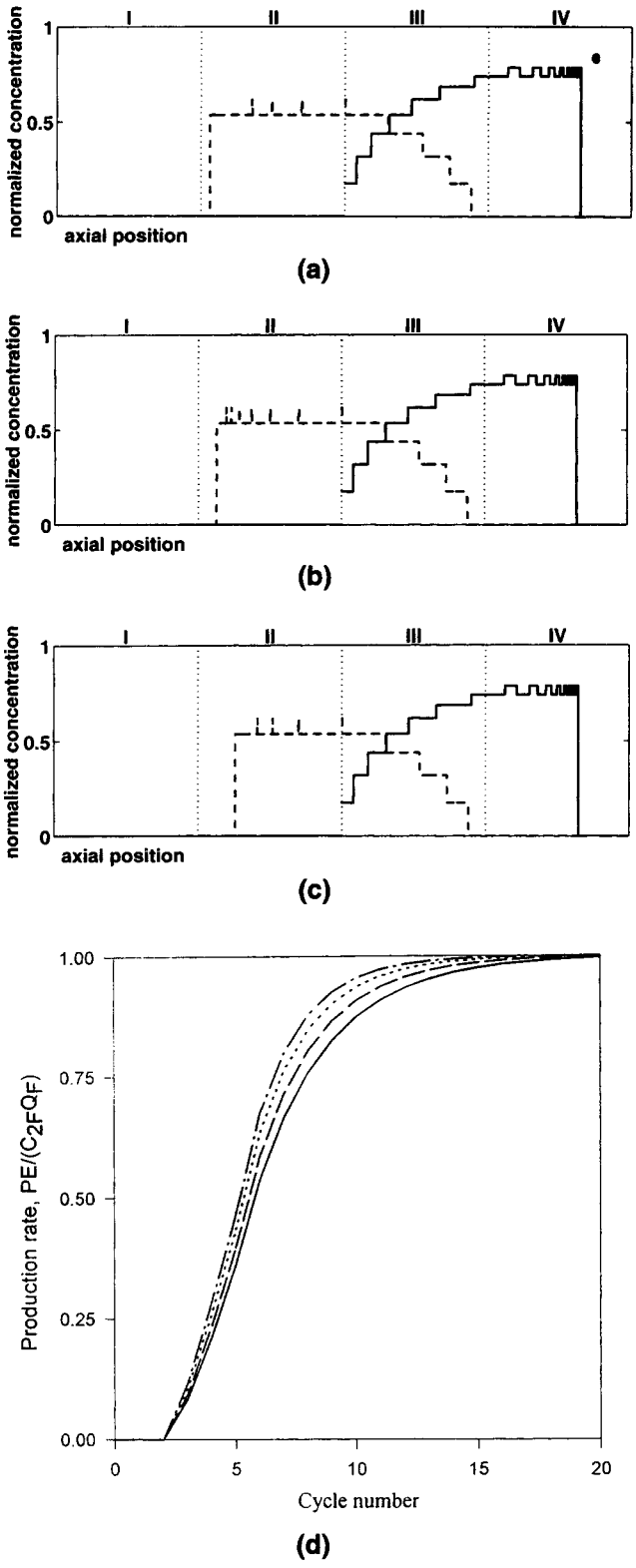

Figure 4. Influence of the liquid flow rate in section I.

Same parameters as in Figure 2, except for β_1, which takes different values. (a) Axial concentration profiles under steady-state conditions, $\beta_1 = 1.05$. (b) Axial concentration profiles under steady-state conditions, $\beta_1 = 1.1$. (c) Axial concentration profiles under steady-state conditions, $\beta_1 = 1.3$. (d) Production rate of the extract. $\beta_1 = 1.05$, solid line; $\beta_1 = 1.1$, dashed line; $\beta_1 = 1.2$, dotted line; $\beta_1 = 1.3$, dash-dotted line.

$$PR(n_r + m) = (1 - K_B^m)C_{1,F}Q_F + K_B^m PR(n_r) \quad (17a)$$

$$PE(n_e + m) = (1 - K_C^m)C_{2,F}Q_F + K_C^m PE(n_e). \quad (17b)$$

We can see that as both K_B and K_C are smaller than unity, the production rates tend toward the respective feed rates when m increases indefinitely.

Discussion and Illustrations of the Flow Rate Influence

The influence of the performance of an SMB of unrelated changes in the flow rates in its different sections can now be discussed. Previously, it was only possible to discuss these changes at constant value of β, a condition that is no longer necessary. The following values of the parameters of the separation will be used for illustrations: slopes of the linear isotherms, $K_1 = 2.0$, $K_2 = 4.0$; separation factor, $\alpha = 2$, an easy separation, phase ratio, $F = 0.5$. The abscissa in the figures gives an axial position normalized to the column length. The raffinate and extract concentrations are normalized with respect to the feed concentration, and a 1:1 mixture is considered in the feed—all that without loss of generality.

Same flow rate ratio β

The algebraic solution of the SMB system, generalized by Eqs. 10 and 12, is formally the same as the one previously obtained (Zhong and Guiochon, 1996), except for differences in the definitions of the flow-rate ratios and the introduction of a different value of β_j in each section. Obviously, if we set $\beta_j = \beta$, $\forall j$, these ratios and the positions of each step are exactly those derived in our previous study (e.g., Figures 2 and 3, with $\beta = 1.2$). For an easy understanding of the following results, it should be remembered that β_1 and β_2 represent the ratios of the liquid phase to the solid-phase flow rates in these sections, while β_3 and β_4 are the inverse ratios (see discussion above Eqs. 6a–6d).

The important properties of the algebraic solution were discussed in detail in previous studies (Zhong and Guiochon, 1996). It is useful to summarize the results that can be affected by the use of different values of β_j, that is, by uncorrelated changes of the flow rates in the four sections:

- Steady-state concentration profiles are reached first in section III, when no new concentration plateaus of the raffinate and the extract can be formed in this section during a new cycle. The raffinate reaches this steady-state condition always later than the extract. In Figure 3, the raffinate reaches it at the seventh cycle, while the extract has reached it at the fifth cycle, as indicated by their corresponding numbers of plateaus in section III.
- The steady state can be reached only in an asymptotic sense in section IV, for the raffinate concentration profile, and in section II for the extract (in the ideal case, the separation is always complete). Distance from steady state can be measured by the asymptotic bandwidths given by Eqs. 13, or more accurately by the production rates represented by the dotted lines in Figure 4d for the extract and in Figure 5c for the raffinate.

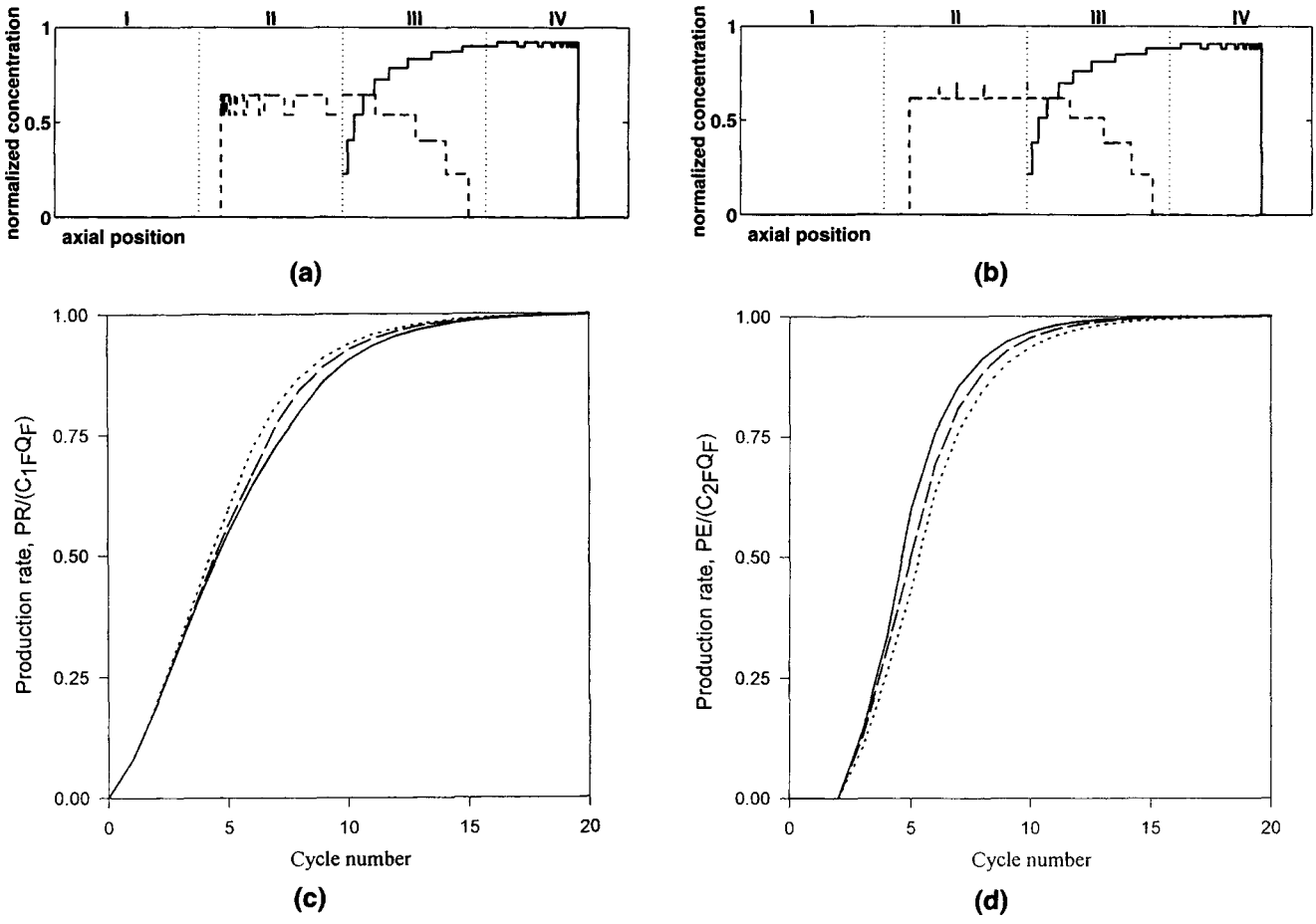

Figure 5. Influence of the liquid flow rate in section II.

Same parameters as in Figure 2, except for β_2, which takes different values. (a) Axial concentration profiles under steady-state conditions, $\beta_2 = 1.06$. (b) Axial concentration profiles under steady-state conditions, $\beta_2 = 1.1$. (c) Production rate of the raffinate. $\beta_1 = 1.06$, solid line; $\beta_1 = 1.1$, dashed line; $\beta_1 = 1.2$, dotted line. (d) Production rate of the extract. $\beta_1 = 1.06$, solid line; $\beta_1 = 1.1$, dashed line; $\beta_1 = 1.2$, dotted line.

• A square-wave oscillation takes place on the concentration plateaus in columns IV or II, as shown in Figure 3 if the equality in Eq. 14 does not take place.

Effect of the flow rate (β_I) in section I

In this case, the flow rates in all three sections, II, III, and IV, are kept constant ($\beta_2 = \beta_3 = \beta_4 = 1.2$), while the flow rate in section I (β_1) is varied. To change the flow rate Q_I, we must change the solvent flow rate and/or the extract flow rate. Figures 4a, 4b, and 4c illustrate the results obtained in this case, with $\beta_1 = 1.05$ (Figure 4a), 1.1 (Figure 4b), and 1.3 (Figure 4c). Obviously, a flow-rate change in section I influences only the position of the extract front in section II. By definition, β_1 is proportional to the liquid phase flow rate in the first section, as mentioned earlier. So, when β_1 increases, the liquid flow rate increases too, the extract front moves faster in section I, when, at the beginning of a new cycle, the extract that is in section II at the end of a cycle is switched back into section I. This faster migration in section I leads to an earlier arrival of the front in section II and to a narrower band of extract in section II. The L_n^d, Λ_n^d, and Λ_∞^d are shorter.

From Eqs. 9 and 10, we see that the plateau concentrations, C_i^{nt*}, are independent of β_1 (K_A does not depend on β_1). So, all the step concentrations in the staircases are independent of the liquid flow rate in section I. This is why no concentration changes are observed in Figures 4a, 4b and 4c.

From Eqs. 9, 11 and 12, we see that only K_C depends on β_1. Accordingly, only the distances L_n^d, Λ_n^d, and Λ_∞^d depend on β_1. This parameter influences only the position of the different steps in the rear concentration profile of the extract, in section II. When β_1 increases, K_C decreases and the asymptotic migration distance of the extract profile in section II (Eq. 13b) decreases, too. This explicitly and quantitatively explains the changes observed when comparing Figures 3, 4a, 4b and 4c.

Even though increasing β_1 decreases the extract bandwidth in section II, it increases the production rate of the extract because of largely increased extract flow rate, as shown in Figure 4d. By contrast, the production rate of the raffinate remains independent of β_1. It is represented by the dotted line in Figure 5c for all three β_1 values.

Effect of flow rate (β_2) in section II

A change of the liquid flow rate in section II requires the appropriate changes of the flow rates of the extract and feed. The results obtained are illustrated in Figures 3, 5a and 5b, with $\beta_2 = 1.06$ (Figure 5a), 1.1 (Figure 5b), and 1.2 (Figure 3). We note also that both K_A and K_C depend on β_2 and will change, both increasing with increasing β_2, that is, with increasing flow rate.

As explained earlier, when β_2 increases, the fluid flow rate increases, so the rear of the extract concentration profile in section II moves slightly farther in the direction of the liquid-phase flow. Thus, the band becomes narrower. A change is not important because the rear of the extract band spends less time in section II than in section I. A quantitative result is easily derived from Eq. 13b. It shows that, when β_2 increases from 1.06 to 1.2, the asymptotic position Λ_∞^d decreases by approximately 4%. On the other hand, a change of β_2 has no influence at all on the position of the raffinate profile. This is illustrated in Figures 3 and 5. It also results from the fact that neither L_0^a (Eq. 11a) nor K_B (Eq. 9b), which both determine the position of the raffinate profile, depends on β_2.

By contrast, the concentrations of the two components decrease markedly with increasing value of β_2. This is explained by Eqs. 9 to 12. Since K_A increases with increasing β_2, the concentration of each step decreases (Eq. 10). Physically, the decrease of the profile concentrations is explained by the increasing dilution of the feed components resulting from the larger liquid flow rate in section II.

The production rate of the raffinate increases with increasing β_2, because of the larger raffinate withdrawal flow rate. On the other hand, the extract production rate decreases because increasing β_2 causes an increase of the extract flow rate, which does not compensate for the decrease of its concentration. These effects are illustrated in Figures 5c and 5d.

Effect of flow rate (β_3) in section III

The results obtained are in Figures 3 ($\beta_3 = 1.2$), 6a ($\beta_3 = 1.02$), and 6b ($\beta_3 = 1.1$). They are similar to those arising from a change in the value of β_2, but now they affect more the raffinate than the extract. For example, the position of the extract profile in section II is independent of the value of β_3. As in the previous case, the concentrations of both components are reduced by an increase in β_3. However, the mechanism is now different. When β_3 increases, the liquid-phase flow rate decreases in section III (the opposite of what happens when β_2 increases) and this is achieved by decreasing the feed flow rate and increasing the raffinate drawoff flow rate. When this happens, the raffinate band becomes shorter and the dilution of the feed components is easily understood.

The opposite conclusions to β_2 are obtained in Figures 6c and 6d for the production rates in function of β_3. This is, in fact, normal because of the opposite effect of β_3 on the liquid-phase flow rate to β_2.

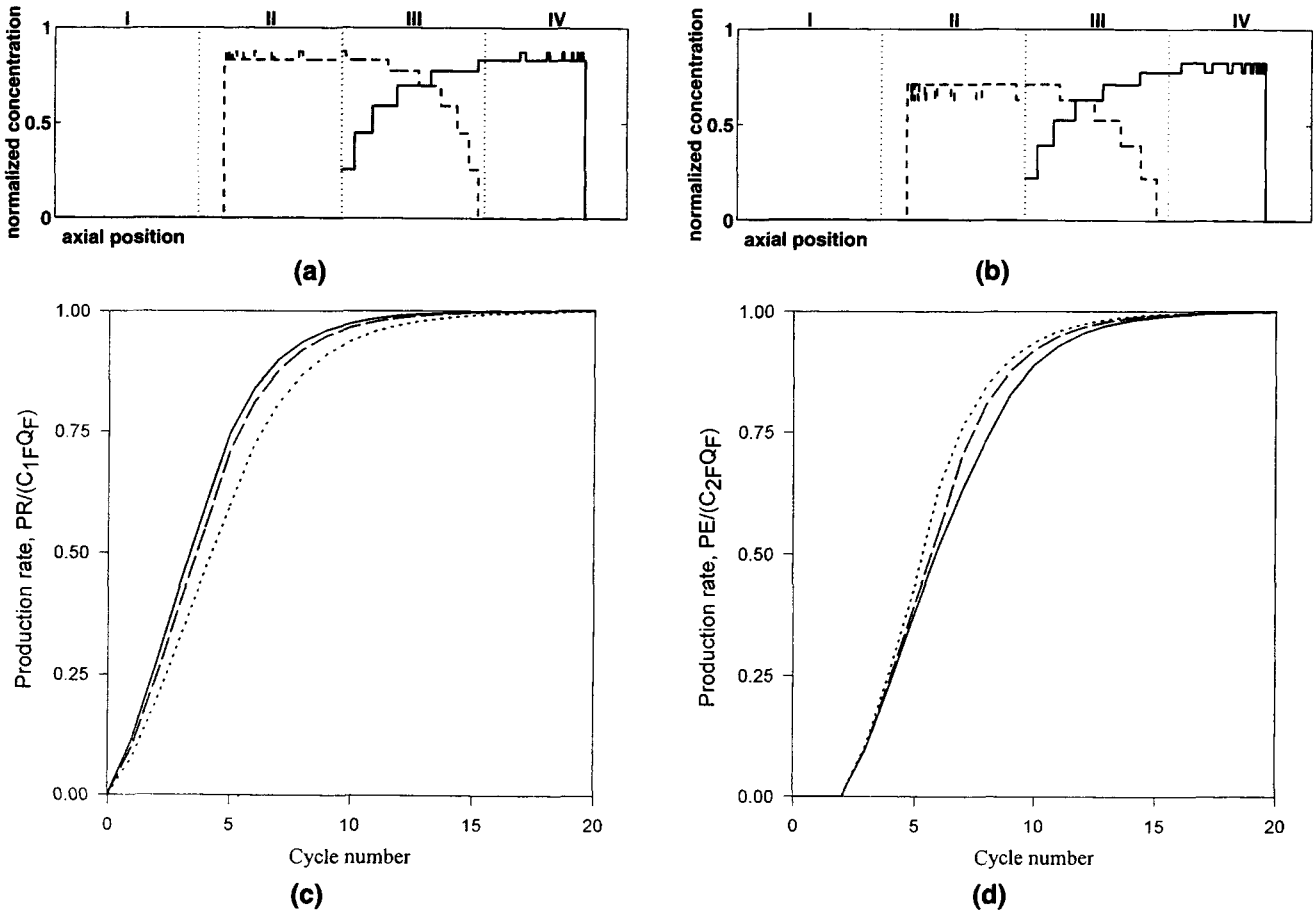

Figure 6. Influence of the liquid flow rate in section III.

Same parameters as in Figure 2, except for β_3, which takes different values. (a) Axial concentration profiles under steady-state conditions, $\beta_3 = 1.02$. (b) Axial concentration profiles under steady-state conditions, $\beta_3 = 1.1$. (c) Production rate of the raffinate. $\beta_1 = 1.02$, solid line; $\beta_1 = 1.1$, dashed line; $\beta_1 = 1.2$, dotted line. (d) Production rate of the extract. $\beta_1 = 1.02$, solid line; $\beta_1 = 1.1$, dashed line; $\beta_1 = 1.2$, dotted line.

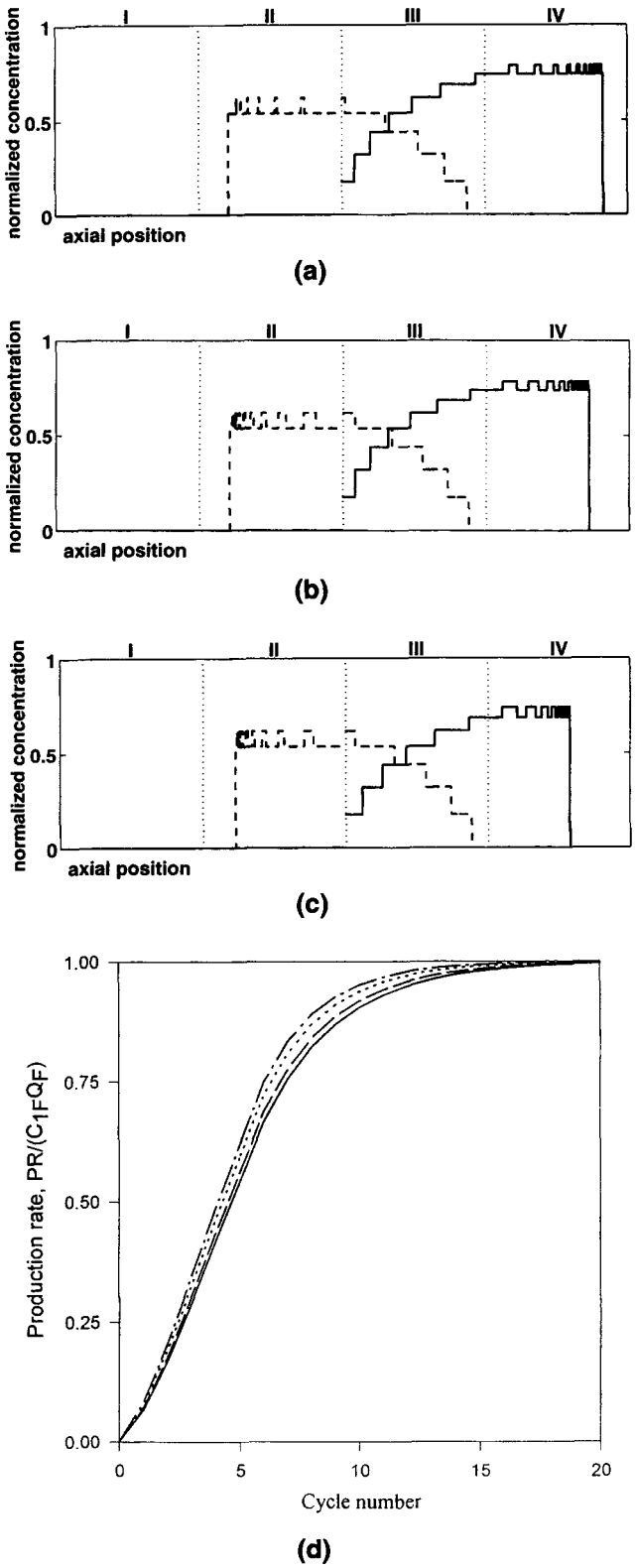

Figure 7. Influence of the liquid flow rate in section IV.

Same parameters as in Figure 2, except for β_4, which takes different values. (a) Axial concentration profiles under steady-state conditions, $\beta_4 = 1.02$. (b) Axial concentration profiles under steady-state conditions, $\beta_4 = 1.1$. (c) Axial concentration profiles under steady-state conditions, $\beta_4 = 1.3$. (d) Production rate of the raffinate. $\beta_1 = 1.02$, solid line; $\beta_1 = 1.1$, dashed line; $\beta_1 = 1.2$, dotted line; $\beta_1 = 1.3$, dash-dotted line.

Effect of flow rate (β_4) in section IV

Figures 7a, 7b and 7c illustrate the consequences of changing the value of β_4 from 1.02 to 1.1 and 1.3, respectively. The situation is similar to the one observed in the case of changes in the value of β_1 (case 2), but the changes take place in section IV. When β_4 increases, the liquid flow rate in section IV decreases and the raffinate bandwidth decreases because its front moves more slowly. However, the concentrations of the raffinate and the extract do not change at all. This effect arises because only K_A and L_0^a depend on β_4 and both of them influence only the stepwidth (Eqs. 8b, 10, 11a and 12a), that is, the position of the concentration profile of the raffinate, not that of the extract or the concentrations.

The production rate of the raffinate increases with increasing β_4 because of increasing the withdraw raffinate flow rate, shown in Figure 7d for $\beta_4 = 1.02$, solid line; $\beta_4 = 1.1$, dashed line; $\beta_4 = 1.2$, dotted line; $\beta_4 = 1.3$, dash-dotted line. However, the production rate of the extract is constant and independent of β_4, as illustrated by the dotted line in Figure 6c.

Conclusion

The algebraic solution was originally derived for a linear, ideal SMB system having a single safety factor, β, for the flow-rate ratios in all its four sections. This solution has now been extended to the more general and more practical case in which there are four different values, β_j, one in each section. The study of the new algebraic solution shows some important, practical results. The liquid-phase flow rates in sections I and IV influence only the position of the rear of the extract band and the front of the raffinate band in these two sections, respectively. Increasing these flow rates at constant solid-phase mass flow rate (i.e., constant cycle time) either decreases the length of the extract band in section II or increases the length of the raffinate band in section IV. As a consequence, increasing β_1 (i.e., increasing Q_I) or β_4 (i.e., decreasing Q_{IV}) decreases the distance over which the corresponding band of product (extract or raffinate, respectively) spreads in the corresponding section. This will improve the purity of the drawoff streams by increasing the distances over which the fronts of these bands have to disperse in order for them to reach the other drawoff port.

Changing the liquid-phase flow rate in either of the two central sections, II and III, has more complicated effects. This influences the concentration profiles of both components in the entire system and the position of the front of one of the two bands. Increasing the flow rate in section II (i.e., increasing β_2) decreases the concentrations of the extract everywhere along its profile, in both sections II and III and the concentration of the raffinate along its profile. It also decreases the width of the extract profile in section II, but does not change the position of the raffinate front in section IV. Conversely, increasing the flow rate in section III (i.e., decreasing β_3), increases both concentrations along the two component profiles, but changes only the raffinate position, moving it forward. Thus, the algebraic solution of a simple model of SMB allows a deeper understanding of the operation of this process. The conclusions of this work are confirmed by experimental results, justifying their application to optimize the experimental conditions of a separation (Yun et al., 1997b).

Acknowledgments

This work was supported in part by Grant CHE-9201663 of the National Science Foundation and by the cooperative agreement between the University of Tennessee and the Oak Ridge National Laboratory. We acknowledge support of our computational effort by the University of Tennessee Computing Center.

Notation

L = migration distance of a front, cm
p = cycle number
u_s = solid phase flow velocity, m/s
z = axial position, cm
β = margin parameter

Literature Cited

Anon., "FDA's Policy Statement," *Chirality*, **4**, 338 (1992).

Balannec, B., and G. Hotier, "From Batch Elution to Simulated Countercurrent Chromatography," *Preparative and Production Scale Chromatography*, G. Ganetsos and P. E. Barker, eds., Dekker, New York, p. 301 (1994).

Barker, P. E., K. England, and G. Vlachogiannis, "Mathematical Model for the Fractionation of Dextran on a Semi-continuous Counter-current Simulated Moving Bed Chromatograph," *Chem. Eng. Res. Des.*, **61**, 241 (1983).

Broughton, D. B., and C. G. Gerhold, "Continuous Sorption Process Employing Fixed Beds of Sorbent and Moving Inlets and Outlets," U.S. Patent No. 2,985,589 (May 23, 1961).

Broughton, D. B., R. W. Neuzil, J. M. Pharis, and C. S. Brearley, "The Parex Process for Recovering Paraxylene," *Chem. Eng. Prog.*, **66**(9), 70 (1970).

Broughton, D. B., "Production-scale Adsorptive Separations of Liquid Mixtures by Simulated Moving Bed Technology," *Sep. Sci. Technol.*, **19**, 723 (1985).

Ching, C. B., and D. M. Ruthven, "An Experimental Study of a Simulated Countercurrent Adsorption System: I. Isothermal Steady State Operation," *Chem. Eng. Sci.*, **41**, 877 (1985).

Helfferich, F., and G. Klein, *Multicomponent Chromatography. A Theory of Interference*, Dekker, New York (1970).

Howard, A. J., G. Carta, and C. H. Byers, "Separation of Sugars by Continuous Annular Chromatography," *Ind. Eng. Chem. Res.*, **27**, 1873 (1988).

Johnson, J. A., and R. G. Kabza, "Sorbex: Industrial-scale Adsorptive Separation," *Preparative and Production Scale Chromatography*, G. Ganetsos and P. E. Barker, eds., Dekker, New York, p. 257 (1994).

Küsters, E., G. Gerber, and F. D. Antia, "Enantioseparation of a Chiral Epoxide by Simulated Moving Bed Chromatography Using Chiralcel-OD," *Chromatographia*, **40**, 387 (1995).

Maki, H., "Separation of Glutathione and Glutamic Acid Using a Simulated Moving-bed Adsorber System," *Preparative and Production Scale Chromatography*, G. Ganetsos and P. E. Barker, eds., Dekker, New York, p. 359 (1994).

Ruthven, D. M., and C. B. Ching, "Countercurrent and Simulated Adsorption Separation Processes," *Chem. Eng. Sci.*, **44**, 1011 (1989).

Stinson, S. C., "Chiral Drugs," *Chem. Eng. News*, **73**, 44 (Oct. 9, 1995).

Yun, T., G. M. Zhong, and G. Guiochon, "Simulated Moving Bed under Linear Conditions: Experimental vs. Calculated Results," *AIChE J.*, **43**, 935 (1997a).

Yun, T., G. M. Zhong, and G. Guiochon, "Experimental Study of the Influence of the Flow Rates in SMB Chromatography," *AIChE J.*, **43**, 2970 (1997b).

Zhong, G. M., and G. Guiochon, "Analytical Solution for the Linear Ideal Model of Simulated Moving Bed Chromatography," *Chem. Eng. Sci.*, **51**, 4307 (1996).

Manuscript received Mar. 11, 1997, and revision received July 29, 1997.